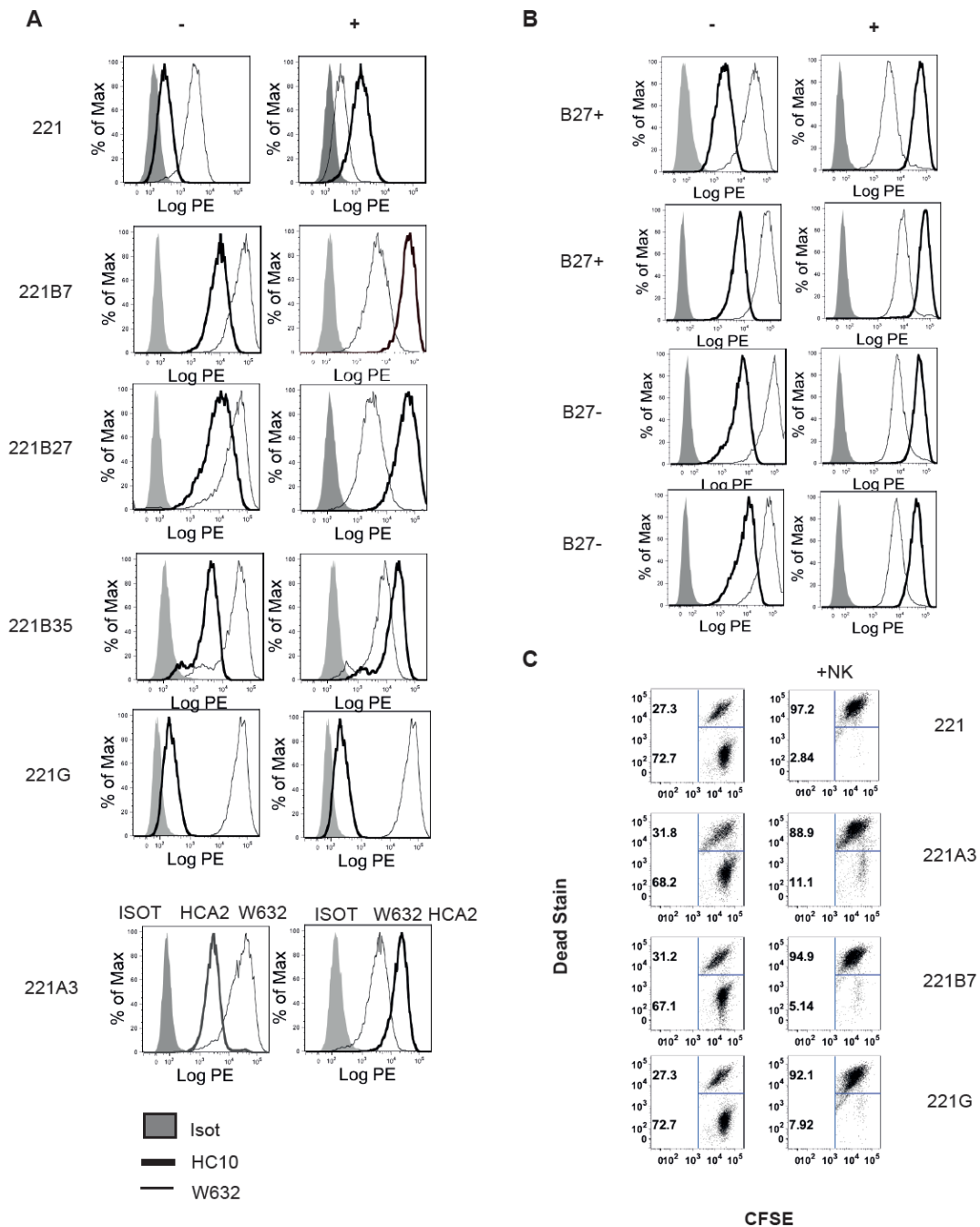


Suppl. Figure 1: The image shows plots interface RMSD against scores for complexes predicted by HADDOCK for the B27 dimer and KIR3DL2. The interface RMSD calculations are taken against a structure generated by alignment of B27 dimer and KIR3DL2 to the structure in PDB 3vh8. The best scoring cluster (Cluster 3) from HADDOCK contains structures with less than 2.5 Å interface RMSD with the structure generated via structural alignment.

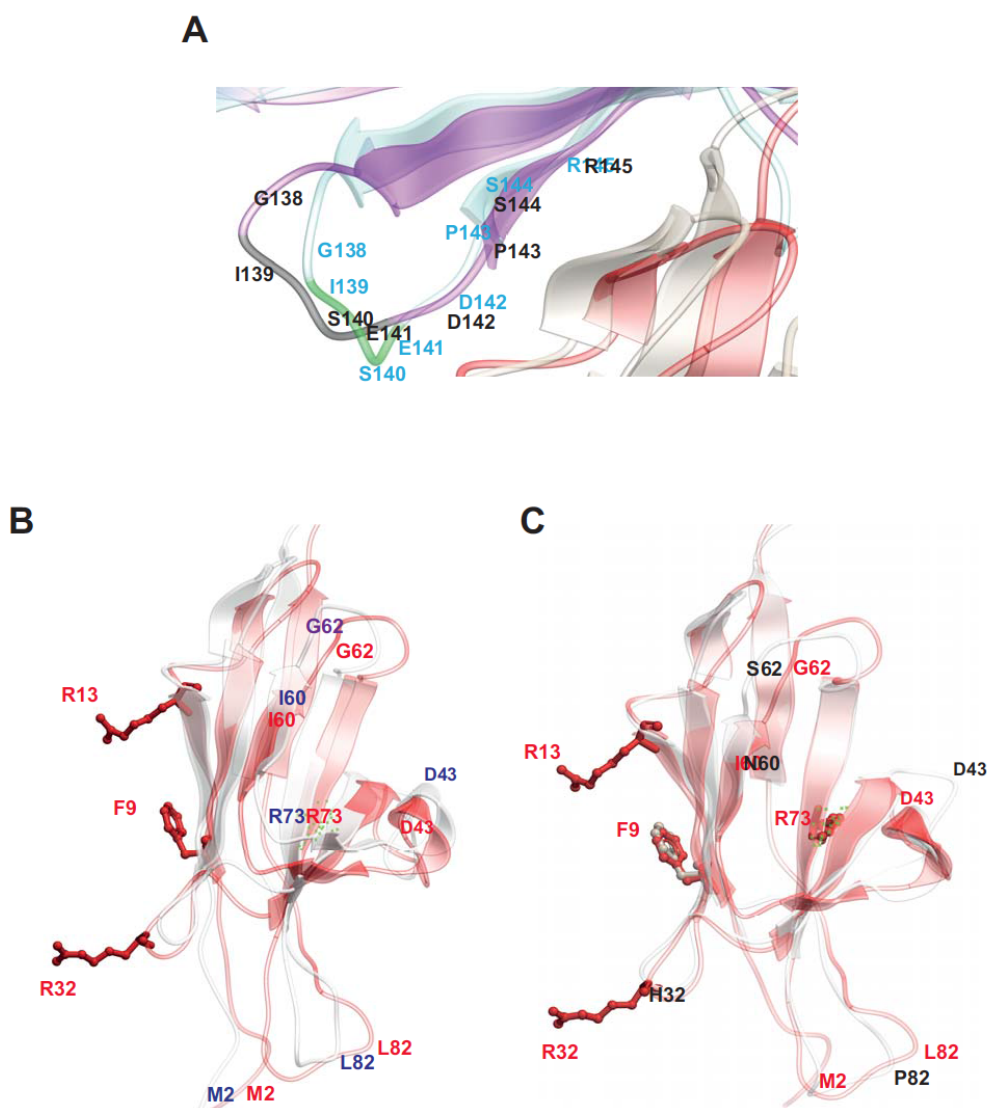


Suppl. Fig. 2A. Representative FACS stain of HLA-class I transfected LCL.721.221 cells before (-) and after (+) acid treatment with the class I antibody W632 and class I heavy chain antibodies HC10 and HCA2. **B** Representative FACS stains of EBV-transformed B cell lines from B27+ and B27-donors before (-) and after (-) acid treatment stained with W632 and HC10 antibodies. Representative stains from 1 of 3 independent experiments. **C** Representative FACS stain of CFSE-labelled parental or transfected LCL.721.221 cells with Dead Stain after 6 hour incubation with or without KIR3DL2+NK cells. Representative stains from 1 of 3 independent experiments.

Table I. Predicted contact residues between HLA-B27 free heavy chain dimers and KIR3DL2. Residues in bold form potential H-bonds.

| B27 Chain | HLA-B27 Residue Number | KIR3DL2 Residue Number | HLA-B27 interface | HLA-B27 Hot Spot | KIR3DL2 Interface | KIR3DL2 Hotspot |
|-----------|------------------------|------------------------|-------------------|------------------|-------------------|-----------------|
| A | GLN54 | ARG73 | 180 | 123 | 180 | 53 |
| A | GLN54 | ARG73 | 180 | 123 | 180 | 53 |
| A | GLN54 | PRO91 | 180 | 123 | 180 | 0 |
| A | ARG62 | GLU141 | 180 | 84 | 180 | 58 |
| A | ARG62 | ASP142 | 180 | 84 | 180 | 0 |
| A | ARG62 | PRO143 | 180 | 84 | 180 | 0 |
| A | ARG62 | SER144 | 180 | 84 | 180 | 95 |
| A | ARG108 | PHE129 | 180 | 175 | 171 | 1 |
| A | ARG108 | GLU130 | 180 | 175 | 180 | 111 |
| A | ARG108 | VAL147 | 180 | 175 | 180 | 180 |
| A | ARG108 | GLY148 | 180 | 175 | 180 | 0 |
| A | ARG108 | VAL147 | 180 | 175 | 180 | 123 |
| A | GLU163 | LEU146 | 180 | 0 | 180 | 180 |
| A | GLU166 | VAL147 | 180 | 180 | 180 | 180 |
| A | ARG169 | GLU130 | 180 | 127 | 180 | 111 |
| A | ARG169 | HIS131 | 180 | 127 | 180 | 41 |
| A | ARG169 | VAL147 | 180 | 127 | 180 | 180 |
| A | ARG170 | ARG145 | 180 | 1 | 180 | 180 |
| AB | GLU177 | ARG44 | 180 | 32 | 180 | 9 |
| A | THR178 | ASP43 | 180 | 32 | 180 | 48 |
| A | GLN180 | ARG44 | 180 | 0 | 180 | 9 |
| A | LYS186 | MET2 | 180 | 0 | 180 | 1 |
| A | LYS186 | GLY3 | 180 | 0 | 179 | 0 |
| A | LYS268 | LEU82 | 180 | 0 | 180 | 17 |
| A | LYS 268 | LEU82 | 180 | 0 | 180 | 17 |
| A | LYS268 | THR83 | 180 | 0 | 180 | 0 |
| B | GLY16 | PHE9 | 180 | 0 | 180 | 6 |
| B | GLY16 | HIS29 | 180 | 0 | 180 | 0 |
| B | GLY16 | PHE34 | 180 | 0 | 180 | 0 |
| B | ARG17 | PHE9 | 178 | 0 | 180 | 6 |
| B | GLY18 | PHE9 | 180 | 0 | 180 | 6 |
| B | GLN72 | MET165 | 177 | 0 | 180 | 0 |
| B | ASP77 | VAL167 | 180 | 0 | 180 | 50 |
| B | THR80 | ILE139 | 180 | 0 | 180 | 101 |
| B | THR80 | VAL167 | 180 | 0 | 180 | 50 |
| B | ARG83 | GLY138 | 180 | 0 | 180 | 0 |
| B | ARG83 | ILE139 | 180 | 0 | 180 | 101 |
| B | SER88 | ARG13 | 180 | 0 | 180 | 0 |
| B | SER88 | GLN27 | 180 | 0 | 158 | 0 |
| B | GLU89 | ARG13 | 180 | 0 | 180 | 0 |
| B | ALA90 | ARG13 | 180 | 2 | 180 | 0 |
| B | ARG145 | SER228 | 180 | 42 | 180 | 1 |
| B | ARG145 | ASP230 | 180 | 42 | 180 | 0 |
| B | LYS146 | PHE276 | 180 | 33 | 180 | 174 |
| B | ALA149 | SER227 | 180 | 177 | 180 | 2 |
| B | ALA150 | LEU199 | 180 | 0 | 180 | 0 |
| B | ALA150 | TYR200 | 180 | 0 | 180 | 169 |
| B | ALA150 | GLU201 | 180 | 0 | 180 | 0 |
| B | ARG151 | GLU201 | 180 | 0 | 180 | 0 |

The number of interface and hot spots indicates the number of times the residue was predicted in 180 snapshots from the tail end of the molecular dynamics simulation.



Suppl Figure 3. Predicted conformational changes in KIR3DL2 upon binding to B27 FHC dimer. **A.** Molecular model of the D1 domain of KIR3DL2 bound to B27 FHC dimer (purple) overlaid on unbound KIR3DL2 (light blue). The positions of key residues in KIR3DL2 for binding to B27 FHC dimer and their relative orientations in the bound and unbound molecules are also indicated in black and blue respectively. **B.** Molecular model of the D0 domain of KIR3DL2 bound to B27 FHC dimer (red) overlaid on unbound KIR3DL2 (white). The positions of key residues in KIR3DL2 for binding to B27 FHC dimer and their relative orientations in the bound and unbound molecules are indicated in red and dark blue respectively. **C.** Molecular model of the D0 domain of KIR3DL2 bound to B27 FHC dimer (red) overlaid on the D0 domain of KIR3DL1 bound to HLAB57 (white). The positions of key residues in KIR3DL2 for binding to B27 FHC dimer and their relative orientations to residues in the bound KIR3DL1 molecule are indicated red and black respectively.